ACI STRUCTURAL JOURNAL TECHNICAL PAPER

Title no. 108-S69

Fiber-Reinforced Polymer Bond Test in Presence of Steel and Cracks

by Mehdi Taher Khorramabadi and Chris J. Burgoyne

The understanding of failure modes of flexurally fiber-reinforced polymer (FRP)-strengthened reinforced concrete (RC) beams that initiate away from the beam's end requires a realistic knowledge of the bond behavior between the FRP and the concrete between cracks in the presence of steel. The conventional method used to obtain a bond characteristic is to pull a bonded FRP from a concrete block, which effectively simulates the conditions in the anchorage regions of a strengthened beam. The boundary conditions in the anchorage regions differ significantly from those in the regions between the cracks, so a different model must be used. A new bond test method is proposed and tests are carried out to mimic the conditions in both the cracked and anchorage regions when steel is present. The test results showed that not only do the bond models differ significantly in the cracked and anchorage regions, but also the steel and its bond stress affect the bond behavior.

Keywords: anchorage regions; average bond stress-slip model; bond behavior; cracked regions; fiber-reinforced polymer.

INTRODUCTION

The flexural strengthening of reinforced concrete (RC) beams is achieved by either externally bonding (EB) or near-surface mounting (NSM). In both of these methods, the fiber-reinforced polymer (FRP) bonds longitudinally to the tension face of the beam. Figure 1(a) shows a schematic view of an RC beam flexurally strengthened with an NSM FRP strip. The EB and NSM methods are shown in Fig. 1(b). This study distinguishes between bond behavior in the anchorage region—close to the end of the FRP reinforcement (the FRP-end)—and the behavior away from that zone, which will be termed the "cracked region" (Fig. 1(a)).

The interaction between the FRP and substrate material is a key factor. Premature failures occur when the stress conditions in the FRP or the substrate material exceed the failure criteria of the constituent materials. The prediction of the actual stress conditions in the bonded FRP is required to determine the stress conditions at the interfaces between FRP-epoxy-concrete and in each of the constituent materials.

Conventional bond tests (CBTs) have been performed using many different experimental setups to determine the bond behavior (Fig. 2), the most common of which are single-shear bond tests,[1-3] double-shear bond tests,[4,5] and shear bending bond tests.[6-8] The first two (Fig. 2(a) to (d)) are direct pullout tests, where the FRP is directly pulled out from the concrete block by a tensile force at the loaded-end and is free at the unloaded-end. Figure 2(e) and (f) shows the bond tests in the form of beams.

Double-shear and single-shear pullout tests have been the most popular as a result of their simplicity,[9] but numerical and experimental studies have shown that different test setups and small variations in setup can lead to significantly different test results.[10,11] This shows that details of the stress

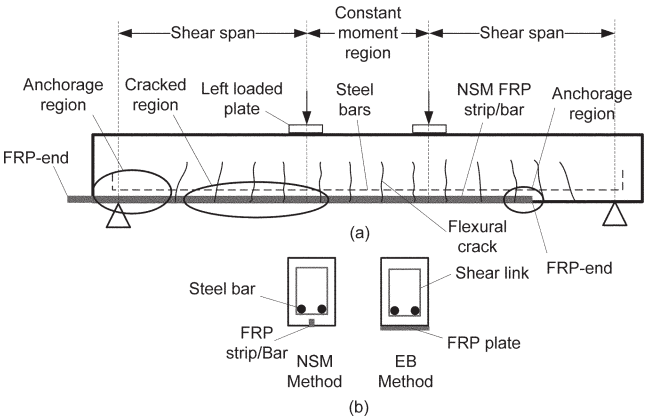

Fig. 1—(a) RC beam strengthened with NSM FRP strip in four-point bending configuration (longitudinal view); and (b) NSM and EB strengthening methods (section view).

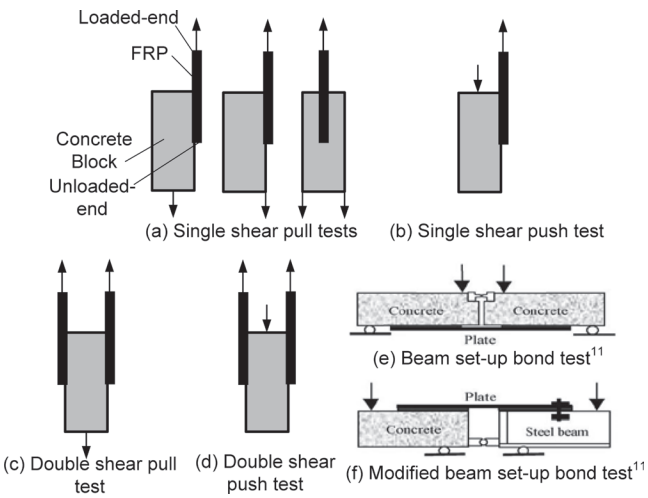

Fig. 2—Classification of bond tests setup.

field in the concrete affect the bond behavior, which in turn means that the boundary conditions of the test are critical.

Therefore, bond tests in the form of beams may better represent the actual conditions than direct pullout tests. In both cases, however, it is conventionally considered desirable to avoid concrete cracks perpendicular to the bonded FRP.

ACI Structural Journal, V. 108, No. 6, November-December 2011.
MS No. S-2010-240 received August 5, 2010, and reviewed under Institute publication policies. Pertinent discussion including author's closure, if any, will be published in the September-October 2012 *ACI Structural Journal* if the discussion is received by May 1, 2012.

Mehdi Taher Khorramabadi *works for Read Jones Christopherson (RJC) Consulting Engineers. He received his PhD in strengthening of concrete structures at the Structures Group, University of Cambridge, Cambridge, UK, in 2010. He received his MS in rehabilitation of structures from Dresden University of Technology, Dresden, Germany, in 2006, and his BS in civil engineering from Amirkabir University, Tehran, Iran, in 2004. His research interests include bond behavior between fiber-reinforced polymer (FRP) and steel and substrate material, strengthening methods of reinforced concrete structures using FRPs, and their failure modes.*

Chris J. Burgoyne *is a Reader in Concrete Structures at the University of Cambridge. He is a member of ACI Committee 440, Fiber-Reinforced Polymer Reinforcement. His research interests include advanced composites applied to concrete structures.*

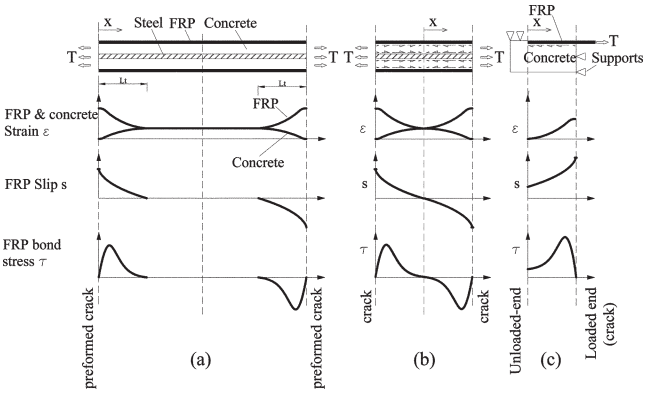

Fig. 3—Strain, slip, and bond stress distributions: (a) before cracking load between two cracks; (b) cracked region at final cracking stage; and (c) anchorage region (similar to CBT).

Thus, even in bond tests in the form of beams, the FRP under consideration is pulled out from one end and is freed from the other end with no crack along the bonded length. Hence, the FRP is effectively tested under the conditions of the anchorage region and not within the cracked regions of a strengthened beam.

These CBTs effectively simulate the conditions at the FRP-end of the strengthened RC beams and do not represent the conditions in the intermediate regions (for example, between cracks). Some researchers[3] have found that the results of CBTs cannot be applied to the cracked regions, and calibrating factors were applied to make the results fit.

A bond test method is proposed herein that mimics the conditions in both the cracked and anchorage regions of a strengthened RC beam. It is shown that the FRP bond behavior in the two regions is significantly different and the presence of steel and the details of its bond stresses directly affect the FRP bond behavior.

RESEARCH SIGNIFICANCE

Bond behavior between FRP-concrete and steel-concrete is usually studied separately, but in an FRP-strengthened RC beam, all three materials interact throughout the beam. The new method mimics conditions in both the cracked and anchorage regions. Cracks are accounted for, as is the interaction between the FRP and the internal steel, both before and after yield. The tests show that the bond behaviors in the two regions differ significantly and that the presence of steel, its yield condition, and its load state directly affect the bond to nearby FRP. These factors cannot be studied with CBTs and have been overlooked in the current design guidelines.[12,13]

PHILOSOPHY OF PROPOSED BOND TEST METHOD

To date, it has been assumed that the results of the CBTs, which effectively mimic the FRP-concrete bond behavior in the anchorage region of a flexurally FRP-strengthened RC beam, can be applied to the rest of the beam. Although bond stress-slip ($\tau - s$) models can be derived from these tests, the boundary conditions differ from those involved in bond transfer between the cracks. Therefore, such an analysis would be inaccurate because:

- The boundary conditions, and hence the strain, slip, and bond stress distributions in most CBTs, do not comply with the actual conditions between the cracks; and
- Although both the steel and FRP reinforcement control the strain distribution in the concrete, the CBTs ignore the effects of nearby steel bars on the bond behavior. The behavior will be different if the steel is yielding.

Bond behavior between and outside cracks

The mechanism of cracking and bond behavior between two cracks can most easily be understood by considering an RC member subjected to pure tension. A concrete member between two adjacent cracks, reinforced with steel and FRP subjected to uniaxial tension, is shown in Fig. 3(a). The applied load T is carried partly by the concrete, partly by the steel, and partly by the FRP strip. The proportions vary with the distance x from the crack. At the crack, no load is carried by the concrete. Away from the crack, the load in the reinforcement decreases. At a distance L_t (transfer length) away from the crack, the strain in the reinforcement (steel and FRP) is equal to the concrete strain. Beyond this point, the slip and bond stresses are zero. The transfer lengths for FRP and steel may differ. As the load increases, new cracks form when the concrete strain exceeds the concrete cracking strain. The number of cracks increases until a stabilized strain condition is reached.

The final situation between two cracks is shown in Fig. 3(b). At the cracked sections, the tension is carried by the FRP and the steel alone and the strains in the reinforcement attain maximum values. Between cracks, the concrete carries some tension and there is a corresponding reduction in the reinforcement stresses. As a result, the bond must take the stress out of the reinforcement adjacent to a crack and put it back in before the next crack is reached. Between adjacent cracks, the directions of the bond stress and slip reverse and, at one point at least, the bond stress and slip must both be zero.

The conventional way to test the bond properties of reinforcement is to pull a bar from a concrete block, as shown in Fig. 3(c). The differences between the bond behavior in Fig. 3(b) and (c) are clear. In the CBTs, a stress distribution forms with a maximum close to the loaded-end and zero at the unloaded-end (FRP-end). The FRP-end slip is initially zero, but eventually slip propagates through from the loaded-end, even though there is no strain at the FRP-end. This differs from the conditions between the two cracks, where slip remains zero at one point between the two cracks. Bond stress in a CBT is initially zero away from the loaded-end, but eventually stresses develop as the strain propagates through from the loaded-end. Considering that strain at the FRP-end is always zero, the strain difference between the FRP-end and a nearby point produces bond stress in the region close to the FRP-end. This condition is not the same as in the regions between cracks. Thus, the

CBTs do not provide boundary conditions that mimic the behavior between cracks.

Hypothesis of steel effects on bond behavior

The other difference between the behavior of the bonded FRP in a strengthened RC beam and a CBT is an effect due to the presence of the steel. The FRP is being provided to enhance the tensile capacity of a beam, which is presumably deficient. The main tension steel is likely to be at a cover depth from the surface, and the reinforcement is being placed either on the surface or in a groove cut in that cover. The presence of steel is known to affect the strain distribution in concrete (which is why steel is detailed to control the crack widths in beams and slabs). Thus, the strain in the concrete next to the FRP is likely to be affected by the nearby reinforcing bar.

This effect can be expected to alter when the reinforcing bar yields. In these regions, the FRP must be carrying a great share of the load and the variation of that stress along the beam may change when the steel starts to yield. This effect is particularly important when dealing with strengthening because the whole point of the exercise is to increase the moment capacity beyond that of the original beam, so yielding must be expected. The reinforcing bar may also be corroded, which would lower the yielding load. In general, strengthened beams should be designed to ensure that the steel does not yield at the working load, but to have sufficient robustness, the FRP must not debond as soon as the steel yields.

Where the steel has yielded, all variations in the tensile force (either in time or position along the beam) must be carried by the FRP, which leads to an increase in the expected bond stress. It is likely, however, that the steel will yield first at crack locations while remaining elastic between the cracks. For this reason, bond tests were devised that allowed the bond to be studied with and without steel being present.

PROPOSED BOND TEST METHOD

The idea of the proposed bond test is to simulate the tension zone of the beam in the cracked regions both before and after steel yielding, as well as in the anchorage regions. The method considers the effects of the steel on the stress distribution and verifies the compliance of boundary conditions with the conditions of a strengthened RC beam in both the anchorage and cracked regions.

The specimens consisted of concrete ties with rectangular cross sections strengthened with steel bar(s) and carbon fiber-reinforced polymer (CFRP) strips that were laid longitudinally (Fig. 4(a)). Additional anchorage bars were provided in the end regions that extended outside the specimen to connect to the test rig. To ease further referencing to different parts of the specimens, the regions at both ends where the anchored bars were embedded are termed the "anchorage regions" and the region between, without anchored bars, is termed the "central region." Notches as crack inducers were preformed in the central region to simulate the cracked regions. The regions outside the central region mimic the anchorage regions of an RC beam. By increasing the steel in the anchorage regions, the central steel can yield. Thereafter, any load increment would be carried only by the CFRP at the cracked section and by the concrete, CFRP, and steel (if locally unyielded) between two cracks. That mimics the situation in the cracked regions of a strengthened RC beam.

DESIGN, PREPARATION, AND TESTING OF BOND TEST SPECIMENS

Based on the proposed bond test method, five specimens were designed and constructed. One specimen was reinforced only with steel bars, one only with CFRP strips, and three with both (Fig. 4(c)). The lengths of the specimens varied between 1000 and 1100 mm (39 and 43 in.) to provide sufficient anchorage length. Four specimens were constructed with a uniform cross section of 100 x 125 mm (3.9 x 4.9 in.) over the entire length. One specimen was constructed with a cross section of 100 x 62 mm (3.9 x 2.4 in.) to simulate part of a specific beam cross section in the tension zone between the longitudinal steel reinforcement and concrete cover.

Where applicable, the central reinforcement consisted of one or two 10 mm (0.4 in.) steel bars running along the full length of the specimen. The anchorage bars consisted of two 16 mm (0.6 in.) steel bars.

One 1.2 x 12 mm (0.05 x 0.5 in.) CFRP strip was embedded in each of the two precast 5 x 14 mm (0.2 x 0.6 in.) grooves and was extended 20 mm (0.8 in.) outside the specimens to allow the end slip to be measured. The grooves were cast by placing wooden strips at the sides of the formwork.

The specimens were coded for identification in the following format: Bd-n_sSn_f F-f_{cu}, where Bd, S, and F stand for bond test series, steel bars, and FRP strips, respectively. The variables n_s and n_f are the number of steel bars and CFRP strips in the central region, respectively; and f_{cu} is the concrete cube strength of the specimen. The specimen details are given in Tables 1 and 2.

To localize the position of the cracks, notches as crack inducers were precast around the section at three locations along the central region of three specimens (Specimens Bd-0S2F-73, Bd-1S2F-92, and Bd-2S2F-75)—two at the ends of the central region and one at the middle. The notches were cast by placing 6 x 6 mm (0.2 x 0.2 in.) wooden strips on the four faces of each section. To investigate the effects of the notches on the stresses and minimum crack spacing, Specimen Bd-1S2F-67 was cast with only two notches at the middle of the central region on the two faces with no FRP strips. Specimen Bd-1S0F-54 was cast with no notch.

Specimens Bd-0S2F-73, Bd-1S2F-92, and Bd-2S2F-75 were fully instrumented (Fig. 4(a) and (b)). This figure also shows the labeling used to identify locations along the specimen ($A \rightarrow O$). The force T and the overall extension were measured within the test machine. The strains were measured in only one central steel bar and one FRP strip in each specimen using 6 mm (0.2 in.) strain gauges. The crack widths at the locations of the notches were measured by two linear resistance displacement transducers (LRDTs) placed on opposite sides of the FRP so that any possible asymmetric displacement could be monitored. FRP-end slips at the ends of the specimens were monitored by LRDTs. The average concrete strains in the high concrete strain regions in the central region were measured by portal gauges.

Uniaxial tensile tests were conducted on the bond test specimens under displacement control at a mean rate of 0.09 mm/s (0.004 in./s). The RC ties were placed vertically in a 2000 kN (450 kips) test machine, as shown in Fig. 4(b). Data were recorded every 0.3 seconds.

TEST RESULTS

The load-elongation behaviors obtained from the cross-load movement of the test machine are shown in Fig. 5.

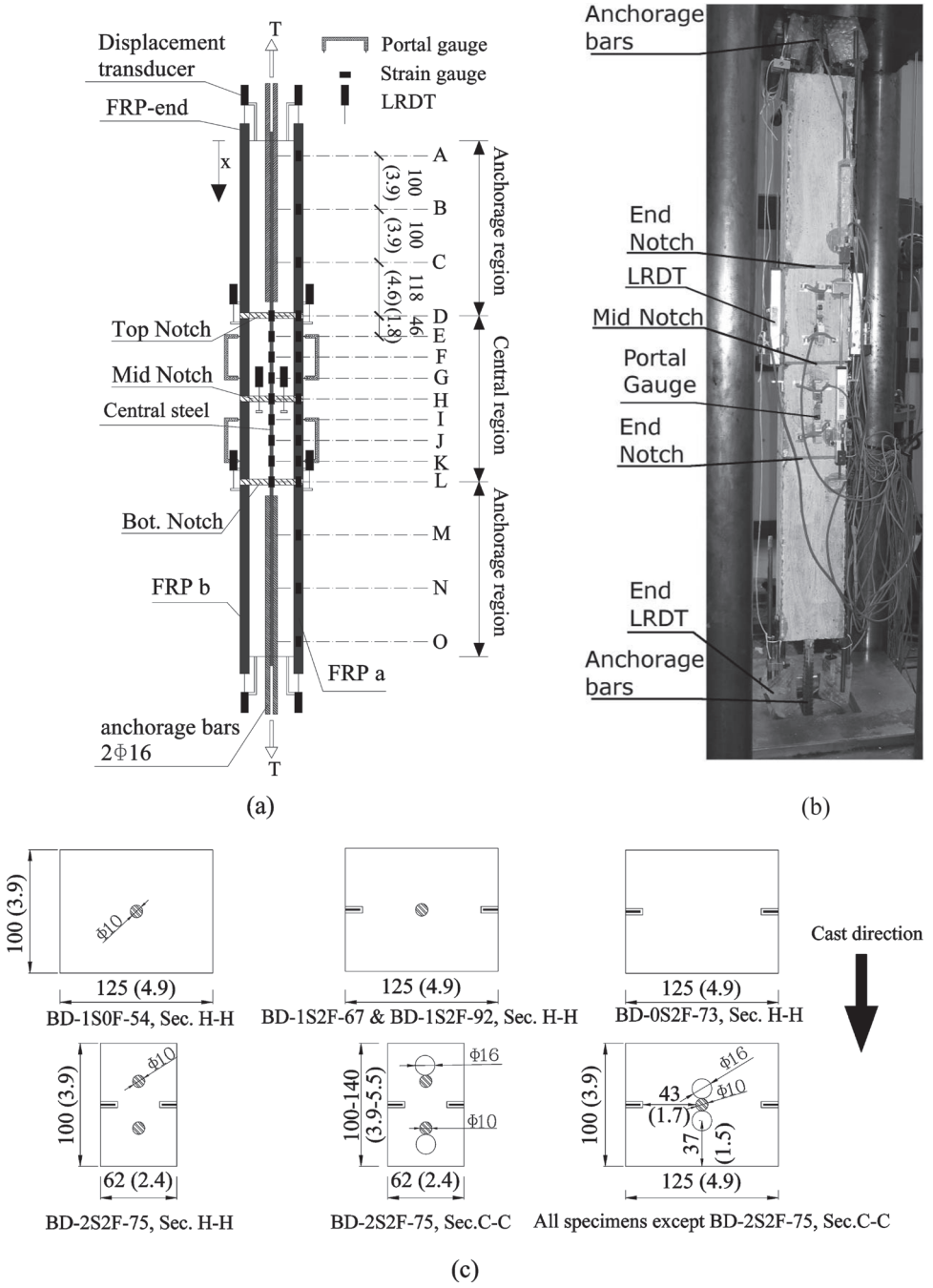

Fig. 4—Bond test series: (a) side view; (b) Specimen Bd-1S2F-92 in test rig; and (c) cross sections. (Note: Dimensions in mm [in.].)

Table 1—Details of bond test specimens

Specimen ID	Central region reinforcement	Cube concrete strength, MPa (ksi)	Central region width x height x length, m (in.)	Anchorage region width x height x length, m (in.)
Bd-1S0F-54	1ϕ10	54 (7.8)	0.1 x 0.124 x 0.300 (3.9 x 4.9 x 11.8)	0.1 x 0.124 x 0.350 (3.9 x 4.9 x 13.8)
Bd-1S2F-67	1ϕ10 + 2 CFRP	67 (9.7)	0.1 x 0.124 x 0.366 (3.9 x 4.9 x 14.4)	
Bd-0S2F-73	2 CFRP	73 (10.6)		
Bd-1S2F-92	1ϕ10 + 2 CFRP	92 (13.3)		
Bd-2S2F-75	2ϕ10 + 2 CFRP	75 (10.9)	0.1 x 0.062 x 0.366 (3.9 x 2.4 x 14.4)	Varies from 0.1 x 0.062 x 0.367 to 0.14 x 0.062 x 0.367 (Varies from 3.9 x 2.4 x 14.4 to 5.5 x 2.4 x 14.4) (Fig. 6(e))

Specimen Bd-1S0F-54

The first trial specimen was made to check the initial design. This specimen had one steel bar with no CFRP strip, but the longitudinal grooves were cast along the specimen. No notch was cast around the sections.

Figure 5 shows that the specimen behaved elastically up to 40 kN (9 kips) with 11 mm (0.4 in.) elongation, after which it became plastic when the steel yielded. The failure occurred at 46.8 kN (10.5 kips) by steel rupture with 67 mm (2.6 in.) elongation. The specimen acted as a steel tension member surrounded by concrete.

Figure 6(a) shows the specimen after failure. The two horizontal lines locate the border between the anchorage regions and the central region. The numbers on the specimens present the loads in kN (kips) at which the cracks were observed. Only two cracks formed along the specimen—240 mm (9.4 in.) apart—one at the edge of the central region and one in the central region.

Specimen Bd-1S2F-67

This trial specimen was reinforced with one central steel bar and two CFRP strips in the central region. Notches were cast on only two faces at Section H-H (labeled in Fig. 4(a)) and no notches were cast elsewhere.

Figure 5 shows that the initial response was generally linear-elastic until the steel yielded at approximately 60 kN (13.5 kips) when the stiffness reduced. The response became nonlinear when debonding began and new cracks formed. The specimen failed just before the debonding reached the end of the anchorage region. The failure occurred as a result of the end anchorage splitting at approximately 90 kN (20 kips).

Figure 6(b) shows the specimen after failure. The first visible crack formed at approximately 20 kN (4.5 kips) at Mid-Notch H only on one face, which was then followed by second and third cracks at Sections L and D, respectively. At approximately 30 kN (6.7 kips), the crack at Notch H was completely formed but did not open, unlike the other sections (Sections L and D). At approximately 65 kN (14.6 kips), debonding initiated from Crack H in the central region and from Cracks L and D in the anchorage regions at the epoxy-concrete interface.

Specimen Bd-0S2F-73

Specimen Bd-0S2F-73 was reinforced with only two CFRP strips and without any steel bar in the central region. The notches were cast around three sections in the central region (Sections D-D, H-H, and L-L). Figure 5 shows that the specimen generally behaved linear-elastically up to failure and acted as a CFRP tension member bonded to concrete.

Figure 6(c) shows the specimen after failure. The first visual crack was observed at approximately 20 kN (4.5 kips) at the bottom notch L. As the load was increased, second and third cracks formed at the H and D notches, respectively. Between 20 and 33 kN (4.5 and 7.4 kips), herringbone cracks formed in the concrete along the central region of the specimen on both sides of the faces where the CFRP strips were embedded. The formation of these cracks reduced the bond stresses and caused a gradual reduction in the stiffness. At approximately 32 kN (7.2 kips), one diagonal secondary crack formed in each of the anchorage regions away from the notches. At approximately 38 kN (8.5 kips), debonding started from the toe of these secondary cracks toward the ends of the specimen, primarily at the FRP-epoxy and epoxy-concrete interfaces. The debonding propagated into the anchorage region and the specimen failed at 51 kN (11.5 kips) as soon as the debonding reached the end of the specimen.

Table 2—Details of bond test specimens

Reinforcement	Young's modulus, GPa (ksi)	Strength, MPa (ksi)
CFRP	165 (23,900)	2800 (406) Rupture
Steel	200 (29,000)	600 (87) Yielding

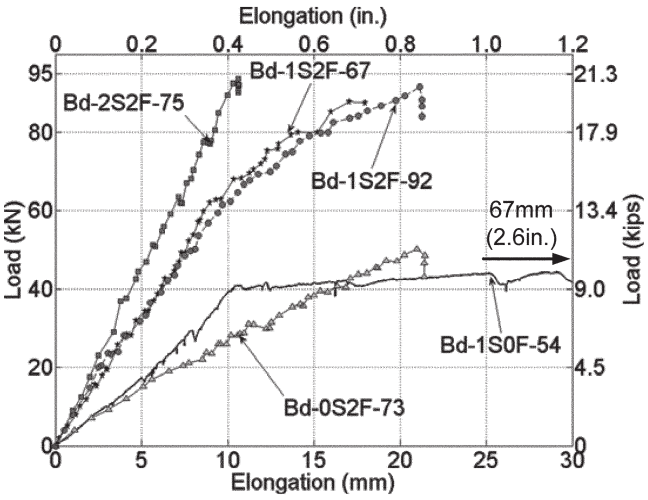

Fig. 5—Comparison between total load versus overall elongation of bond test specimens.

Fig. 6—Specimens after failure: (a) Specimen Bd-1S0F-54; (b) Specimen Bd-1S2F-67; (c) Specimen Bd-0S2F-73; (d) Specimen Bd-1S2F-92; and (e) Specimen Bd-2S2F-75. (Note: Numbers on specimens in kN; 1 kN = 0.2248 kips.)

Specimen Bd-1S2F-92

As with Specimen Bd-1S2F-67, Specimen Bd-1S2F-92 was reinforced with one central steel bar and two CFRP strips

in the central region. The main differences between the two specimens were the concrete strength and the number of notches. Specimen Bd-1S2F-92 had a higher concrete strength—92 MPa (13.3 ksi) compared to 67 MPa (9.7 ksi). The notches were cast around three sections (Sections D-D, H-H, and L-L) in the central region of Specimen Bd-1S2F-92.

The initial response in the load-elongation plot was generally linear-elastic until the steel yielded at approximately 60 kN (13.5 kips). The stiffness reduced post-steel yielding and the cracks at the notches widened. Figure 6(d) shows the specimen after failure. Small wedges initiating from 55 kN (12.4 kips) formed at both sides of each notch. The response remained generally linear up to 80 kN (18 kips). The response became nonlinear when debonding began. At approximately 76 kN (17 kips), the diagonal cracks between the yielded and unyielded regions formed in the concrete in the anchorage regions. Then, the debonding propagated from the toe of the secondary crack toward the specimen's end in the top anchorage region at the epoxy-concrete interface. The specimens failed as soon as the debonding reached the end of the anchorage region at approximately 90 kN (20 kips) load.

Herringbone crack formation started on both sides of the faces where CFRP strips were embedded. They initiated at approximately 70 kN (15.7 kips) along the central region and stabilized at approximately 85 kN (19 kips). This specimen was similar to Specimen Bd-1S2F-67, which had a lower concrete strength and had no notch on the faces where CFRP strips were bonded. No herringbone cracks formed in the specimen without a notch (Fig. 6(b)), but debonding propagated in the central region. Where herringbone cracks formed in the central region, no debonding was observed (Fig. 6(d)). A similar comparison can be made between the anchorage and central regions of each specimen. In the regions where herringbone cracks formed, debonding did not initiate or was delayed to a higher load level. This shows one of the effects of the notches (cracks) on the bond stresses.

The response of Specimen Bd-1S2F-92 is compared with Specimen Bd-1S2F-67 in Fig. 5. Both specimens behaved in a similar way. Specimen Bd-1S2F-92 failed at a slightly higher load than Specimen Bd-1S2F-67, however, possibly due to the higher concrete strength and a delay in the formation of debonding.

Specimen Bd-2S2F-75

This specimen was reinforced with two steel bars in the central region and CFRP strips. Notches were cast all around at three sections (Sections D-D, H-H, and L-L).

Figure 5 shows that the response of this specimen was generally linear-elastic. The specimen failed by splitting of the anchorage region when the central steel was at approximately 98% of the yielding strain.

Figure 6(e) shows the specimen after failure. No visible debonding occurred between the CFRP and substrate material in the central region. The specimen cracked midway between the notches.

It was observed in these tests that if notches were present on the surfaces where the CFRP was placed, then herringbone cracks formed and conventional debonding did not occur.

AVERAGE BOND STRESS-SLIP RELATIONSHIP

There are different methods to find the average bond stress-slip ($\tau - s$) relationship from the experimental test results, most of which require force and slip to be known at two points along the bonded length. The shear stress is taken as a constant value between the two points and the slip is taken as the value at one representative point, often midway between the two locations.

Equilibrium equations can also be established to describe the relationship (Eq. (1)) between the strain in the FRP strip and bond shear stress τ acting at the FRP-substrate interface

$$\tau = \frac{EA}{\Sigma_p}\frac{d\varepsilon}{dx} \tag{1}$$

where $d\varepsilon$ is the change in strain over dx; and Σ_p is the effective perimeter of the section at which the bond stress is calculated. The variables E and A are the modulus of elasticity and the area of the material under consideration, respectively.

The average bond strengths are calculated on the debonded surfaces. As observed in the bond tests, the debonded surfaces were either at the FRP-epoxy or epoxy-concrete interfaces, so two different values for Σ_p can be considered.

If debonding occurs at the epoxy-FRP interface

$$\Sigma_{p1} = t_f + 2h_f \tag{2}$$

If debonding occurs at the epoxy-concrete interface

$$\Sigma_{p2} = t_g + 2h_g \tag{3}$$

where t_f, h_f, t_g, and h_g are the FRP strip thickness, FRP strip width, groove width, and groove height, respectively.

Therefore, the average bond stress can be found using Eq. (1) from strains measured by the gauges. The method to find the slip of the FRP is explained in the following. The resulting $\tau - s$ curve might then be approximated by an analytical relationship (for example, with the least-squares fitting method). Many researchers[14,15] consider the results to be a local bond stress-slip model if the length is fairly short.

Relative slip

The slip $s(x)$ is defined as the relative displacement between the FRP and concrete at a location on their interface with respect to a reference point where the slip is known. Two methods can be applied to calculate the FRP slip at any section shown in Fig. 4(a):

1. Method 1: The slip at any point can be calculated by the integration of the strain functions, which provides the displacement of the FRP and concrete measured from the reference point.[3,16] In the anchorage region, the FRP-end can be considered as the reference point. A displacement transducer can be used to measure the FRP-end slip with respect to the concrete, as shown in Fig. 4(a). The reference point in the central region (between notches) can be taken as a point somewhere between the two cracks where the reinforcement slip is zero and the strain in the reinforcement is minimum compared to the neighboring points. This is the point at which the direction of the bond stress changes due to the load-transfer mechanism between the two cracks.

The central region of the specimen (Fig. 4(a)) between Sections D and L is shown in a more detailed view in Fig. 7. From the measured FRP strain distribution, it was found that

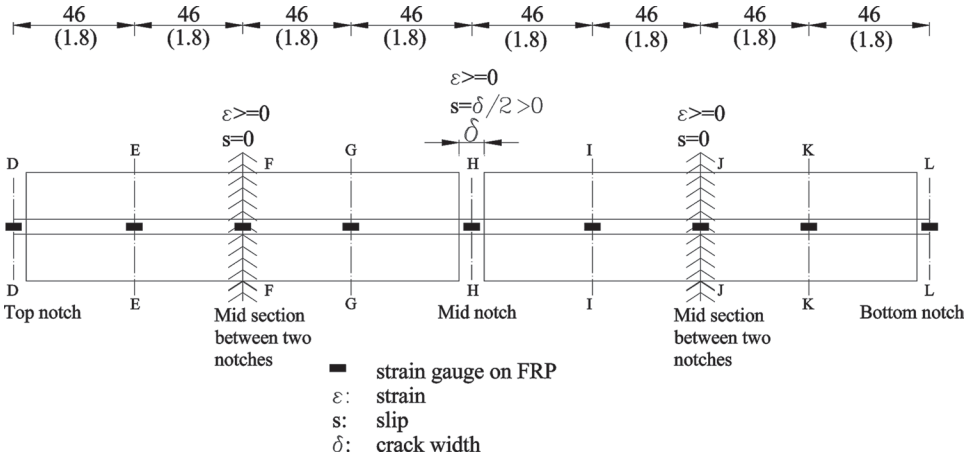

Fig. 7—Central region of specimen with steel and FRP (Specimen Bd-1S2F-92). (Note: Dimensions in mm [in.].)

the FRP strain is minimum at Sections F and J and, therefore, the slip is zero at these locations.[17] The slip at Point H over bonded length FH can be calculated from

$$s_H = s_F + \int_F^H \varepsilon_f(x)dx - \int_F^H \varepsilon_c(x)dx \quad (4)$$

where s_H is the desired slip at Point H; s_F is the known slip at Point F (assumed zero); $\varepsilon_f(x)$ is the FRP strain distribution; and $\varepsilon_c(x)$ is the concrete strain distribution.

The integrations may be performed numerically. Based on the measured local concrete displacement and strains, it was shown[17] that it is reasonable to assume that the concrete displacement is negligible compared to the reinforcement displacement and that the slip at the reinforcement-concrete interface is effectively equal to the reinforcement displacement. It should be emphasized that this assumption does not mean that the concrete strain can be neglected. It was shown previously that in a composite member, the concrete contribution in carrying load is significant. Therefore, the concrete displacement can be neglected compared to the FRP displacement. Thus, the second integral of Eq. (4) will be assumed to be zero in this study.

2. Method 2: The slip between the FRP and concrete on each side of the mid-notch (Section H) may be assumed to be equal to half of the crack width ($\delta/2$) due to symmetry. The crack width δ is measured with displacement transducers at the notch.

Taher Khorramabadi[17] applied these two methods to the same specimens and it was concluded that there is a good agreement between the results of the first and second methods. The calculated slip from strain integration (Method 1), however, was slightly higher than the results measured from the crack width (Method 2) and the difference increased as the load increased.

There are some advantages in the first method, which will be adopted in the subsequent studies:

- There is no need to assume equal slips at both sides of a crack and the slip from each side can be calculated independently;
- The slip can be calculated at other specified locations, not only at the cracked section; and
- In the second method, the displacement transducer has to be placed at the location of the crack before loading, which is not always known.

EXPERIMENTAL AVERAGE BOND STRESS-SLIP RESULTS AND DISCUSSION

In this section, the effects of the presence of steel and position of the bonded regions with respect to the cracks (between or outside cracks) on the average FRP $\tau - s$ relationships are studied. The specimens under consideration were Specimen Bd-1S2F-92, which had both a steel bar and FRP in the central region, and Specimen Bd-0S2F-73, which had only FRP. The two specimens after failure are shown in Fig. 6(c) and (d). As can be seen, the entire anchorage regions AD (top anchorage) and OL (bottom anchorage) of the specimens with steel and without steel debonded, respectively. Herringbone cracks formed in the central regions of both specimens.

The region between each pair of adjacent strain gauges is called a segment. The average bond stress at the epoxy-concrete interface of each segment was calculated from the strain differences at the ends of the segment (Eq. (1)). The location of the strain gauges is shown in Fig. 4(a). The slip was calculated from the FRP strain integration using Method 1. For example, for Segment HG in Fig. 8(a), the bond stress was calculated from the strain differences between Segments H and G and the slip was calculated from the strain integration over Segment FH.

Consider the behavior in the central region (Fig. 8(a) and (b)). In Fig. 8(b) (without steel), the FRP bond stress increases linearly to the peak, after which it drops off rapidly. In contrast, in Fig. 8(a) (with steel), the bond stress increases to approximately 3 MPa (0.4 ksi), after which it drops to a minimum and then subsequently increases (both at a lower slope). It will be shown that this minimum occurs when the steel yields. The subsequent behavior of Regions HG and GF is significantly different. The average bond stress in the FRP is higher in Region HG, which includes the zone where the steel is straining plastically, in contrast to the Region GF, where the steel is at yield but not deforming to any significant extent.

In general, adding steel increases the ductility of the FRP bond behavior and increases the slip at which the peak bond stress occurs (for example, compare Region HG in Fig. 8(a) with Region HI in Fig. 8(b)).

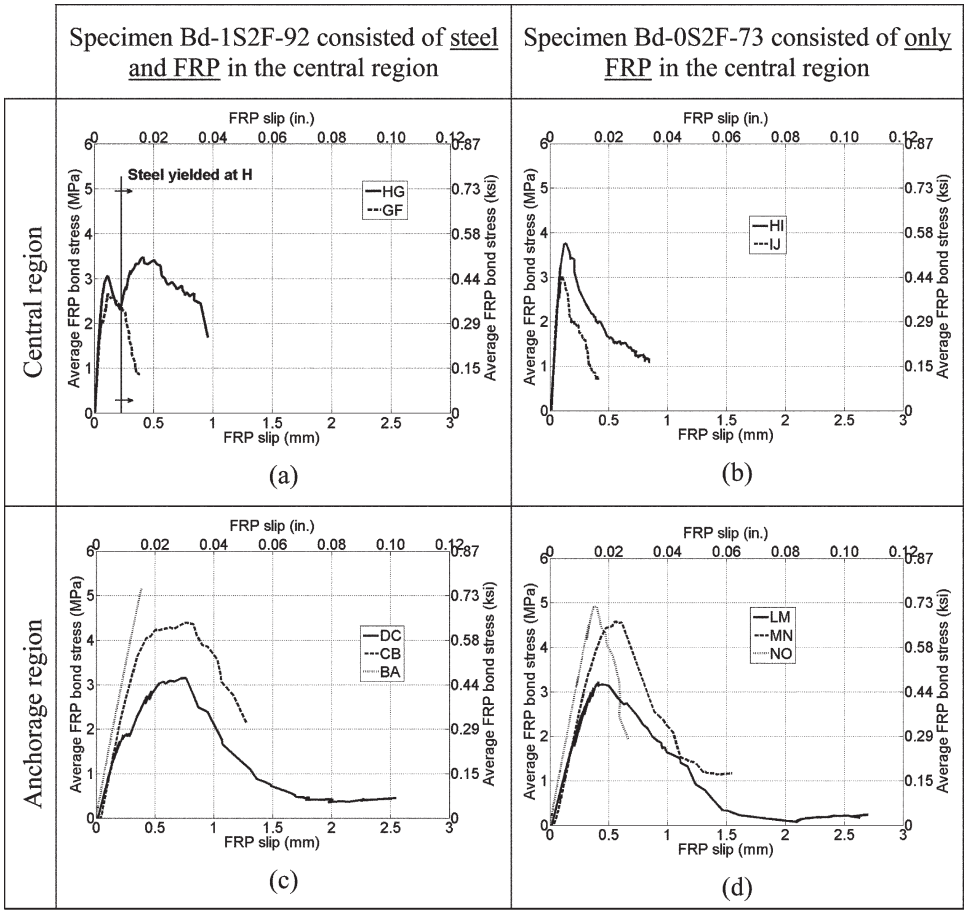

Fig. 8—Average FRP bond stress against FRP slip: (a) Specimen Bd-1S2F-92 in central region; (b) Specimen Bd-0S2F-73 in central region; (c) Specimen Bd-1S2F-92 in anchorage region; and (d) Specimen Bd-0S2F-73 in anchorage region.

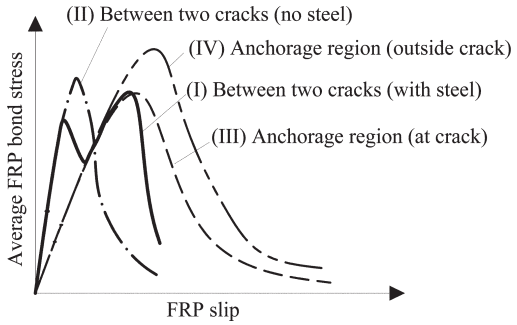

Fig. 9—Effects of location and steel presence on FRP bond stress-slip relationship.

The average $\tau - s$ relationship in the regions in which steel did not yield or did not exist (Fig. 8(b) through (d)) was a typical $\tau - s$ relationship as observed in a CBT, consisting of one ascending branch followed by a descending branch. However, the average $\tau - s$ relationships for specimens with steel in which steel yielded (*HG* in Fig. 8(a)) showed very different behavior. A second ascending and descending branch (which is not observed in CBTs) started when the nearby steel yielded. The stress at which this occurs will be a function of the amount of steel present and, therefore, cannot be regarded merely as a property of the FRP-concrete interface. It is clear that the presence of the tension steel does have a significant effect on the relationship between shear stress and the slip and this should be taken into account when predicting the response of NSM reinforcement.

Regardless of the presence of central steel, the $\tau - s$ relationships in the anchorage regions in Fig. 8(c) and (d) showed higher peak bond stress and more slip compared to the central regions in Fig. 8(a) and (b). The peak average bond stresses in Segments DC and LM (Fig. 8(c) and (d)), which were located at the inner ends of the anchorage regions, however, were lower than in the other segments.

An overview of the results is presented in Fig. 9, which shows a schematic view of the $\tau - s$ relationships between different regions and the effects of steel on these relationships. The initial slope of the rising portion of the average $\tau - s$ relationships was higher between the cracks, regardless of the steel presence (Curves I and II), than in the anchorage regions (Curves III and IV). For the regions between cracks, in cases where steel and FRP were both present (Curve I), the slope of the second ascending portion was equal to the slope of the rising portion in the anchorage regions (Curves III and IV). Thus, after the steel has yielded, the $\tau - s$ relationships followed a curve with a rising slope, as in one of the anchorage regions.

Figures 8 and 9 show that there is no unique average $\tau - s$ model. For example, Fig. 8(a) shows the results of this relationship of two different segments (Segments HG and GF) along the same bonded region (Region FH). Segments HG and GF show the $\tau - s$ relationships at cracked Section H and at a point 46 mm

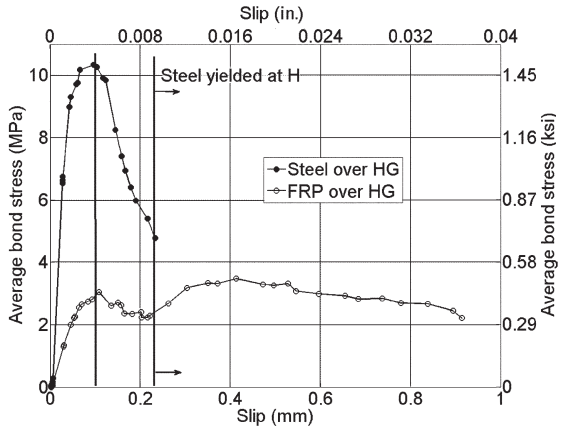

Fig. 10—Connection between average bond stress-slip relationships of steel and FRP in Specimen Bd-1S2F-92 (with steel and FRP).

(1.8 in.) further from Section H, respectively. Comparing these two curves shows that the $\tau - s$ relationships were a function of the distance from the cracked section and the bonded length. Similar conclusions have been reported by *fib* Bulletin No. 40[12] and Nilson.[16]

In conclusion, not only does the steel yielding affect the average FRP $\tau - s$ relationship, but also the bonded length, the position of the segments with respect to the cracks (between or outside cracks), and the distance from the cracks influences these relationships.

CONNECTION BETWEEN STEEL AND FRP AVERAGE BOND STRESSES

The relationship between bond stresses in parallel FRP and steel reinforcement is studied in this section. The average FRP and steel $\tau - s$ relationships in Segment HG of Specimen Bd-1S2F-92 (consisting of steel and FRP) are shown in Fig. 10. The peak average steel bond stress of 10 MPa (1.5 ksi) was obtained between Section H (at the cracked section) and Section G (46 mm [1.8 in.] from Section H).

Although the initial slope for the steel bond stress was higher than that for the FRP bond, the rising and falling of the average FRP bond stress was synchronized with that of the steel. As the slip at Section H increased, both the steel and FRP bond stresses reached peak values at the same slip and then simultaneously both entered into the descending portion. As the steel yielded at Section H, the second ascending portion of the FRP started with a lower slope. Clearly, the presence of steel alters the bond behavior of the FRP, and this effect alters when the steel yields. A similar effect can be observed in a plot of the average bond stresses against total load.

CONCLUSIONS

1. The boundary conditions of CBTs usually used for determining the bond behavior of the FRP-concrete interface mimic the conditions in the anchorage regions of a flexurally FRP-strengthened RC beam, which differ significantly from the conditions in the cracked regions. In addition, these methods usually do not take into account the steel effects on the concrete where the nearby FRP is bonded. Therefore, the results of these bond test methods do not reflect the actual bond behavior in the cracked regions.

2. A new bond test method is proposed herein that mimics the tension region of the beam in the cracked regions before and after steel yielding, as well as in the anchorage regions. The method considers the effects of the steel on the stress distribution and verifies the compliance of boundary conditions with the conditions of a strengthened RC beam in both regions. The central region of the bond specimen mimics the conditions in the cracked regions of a strengthened beam, whereas the anchorage regions of the bond tests simulate the conditions in the anchorage region of a strengthened beam. The boundary conditions in the anchorage regions of the proposed bond test are similar to the CBTs.

3. Based on the experimental bond test results, the presence of steel affects the surrounding concrete strain, which alters the stresses in the nearby bonded FRP, and the yielding of the steel bar alters the strain distribution in the FRP.

4. The experimental bond results showed that there is a connection between the average bond stress-slip relationship of parallel FRP and steel reinforcement in a concrete tie. Although the initial slope for the steel bond stress was higher than that for the FRP bond, the rising and falling of the average FRP bond stress was synchronized with that of the steel. As the steel yielded at a crack and the steel bond stresses dropped to low values, the average FRP bond stress started its second rising portion until the formation of herringbone cracks, beyond which the average FRP bond stress decreased for a second time. Clearly, the presence of steel alters the bond behavior of the FRP, and this effect alters when the steel yields.

5. The experiments showed that the average FRP bond stress-slip relationship is not unique and not only does the steel yielding affect the average bond stress-slip relationships, but also the bonded length, the measured positions with respect to the cracks (between or outside cracks), and the distance from the cracks.

6. It was observed that although no debonding was observed in the cracked regions of a bond specimen with preformed notches, the bond stress reduced after the formation of herringbone cracks. In the anchorage regions of the same specimen, the situation was different; where debonding propagated, no herringbone crack was observed. The central region of the specimen without preformed notches behaved in a similar way to the anchorage regions. In that specimen, debonding formed in its central and anchorage region, and no herringbone crack formed.

7. To successfully predict the debonding behavior of a beam with additional FRP reinforcement, it is necessary to use a bond stress-slip model that has been derived from tests carried out in the presence of steel.

FUTURE WORK

The current design guidelines, such as *fib* Bulletin No. 40[12] and ACI 440.2R-08[13] are based on the CBTs, and hence they take into account neither the crack effects nor the interaction between the nearby steel and FRP of an FRP-strengthened RC beam. With the aid of the proposed test method, Taher Khorramabadi[17] has also shown that the prediction of FRP and steel stresses in a strengthened RC beam based on ACI 440.2R-08[13] may lead to significant differences with the measured values. This is because ACI 440.2R-08[13] only considers FRP-concrete interaction in the anchorage regions, neglecting the presence of the nearby steel and cracks. Further investigations are recommended to consider FRP-concrete-steel interaction in the entire composite

member, separately addressing the bond behavior at the anchorages and elsewhere.

REFERENCES

1. Taljsten, B., "Defining Anchor Lengths of Steel and CFRP Plates Bonded to Concrete," *International Journal of Adhesion and Adhesives*, V. 17, No. 4, 1997, pp. 319-327.

2. Bizindavyi, L., and Neale, K. W., "Transfer Lengths and Bond Strengths for Composites Bonded to Concrete," *Journal of Composites for Construction*, V. 3, No. 4, 1999, pp. 153-160.

3. Teng, J. G. et al., "Debonding Failures of RC Beams Strengthened with Near Surface Mounted CFRP Strips," *Journal of Composites for Construction*, V. 10, No. 2, 2006, pp. 92-105.

4. Yan, X.; Miller, B.; Nanni, A.; and Bakis, C. E., *Characterization of CFRP Bars Used as Near-Surface Mounted Reinforcement*, Engineering Technics Press, Edinburgh, Scotland, 1999.

5. Yoshizawa, H.; Wu, Z.; Yuan, H.; and Kanakubo, T., "Study on FRP-Concrete Interface Bond Performance," *Transactions of the Japan Society of Civil Engineers*, V. 662, No. 49, 2000, pp. 105-119.

6. De Lorenzis, L.; Miller, B.; and Nanni, A., "Bond of Fiber-Reinforced Polymer Laminates to Concrete," *ACI Materials Journal*, V. 98, No. 3, May-June 2001, pp. 256-264.

7. De Lorenzis, L., and Nanni, A., "Characterization of FRP Rods as Near-Surface Mounted Reinforcement," *Journal of Composites for Construction*, V. 5, No. 2, 2001, pp. 114-121.

8. De Lorenzis, L., and Nanni, A., "Bond between Near-Surface Mounted Fiber-Reinforced Polymer Rods and Concrete in Structural Strengthening," *ACI Structural Journal*, V. 99, No. 2, Mar.-Apr. 2002, pp. 123-132.

9. Chen, J. F.; Yang, Z. J.; and Holt, G. D., "FRP or Steel Plate-to-Concrete Bonded Joints: Effect of Test Methods on Experimental Bond Strength," *Steel and Composite Structures*, V. 1, No. 2, 2001, pp. 231-244.

10. Yuan, H. et al., "Full-Range Behavior of FRP-to-Concrete Bonded Joints," *Engineering Structures*, V. 26, No. 5, 2004, pp. 553-565.

11. Yao, J.; Teng, J. G.; and Chen, J. F., "Experimental Study on FRP-to-Concrete Bonded Joints," *Composites. Part B, Engineering*, V. 36, No. 2, 2005, pp. 99-113.

12. *fib* Bulletin No. 40, "FRP Reinforcement in RC Structures," 2007.

13. ACI Committee 440, "Guide for the Design and Construction of Externally Bonded FRP Systems for Strengthening Concrete Structures (ACI 440.2R-08)," American Concrete Institute, Farmington Hills, MI, 2008, 76 pp.

14. Aiello, M. A., and Leone, M., "Interface Analysis between FRP EBR System and Concrete," *Composites. Part B, Engineering*, V. 39, No. 4, 2008, pp. 618-626.

15. De Lorenzis, L.; Rizzo, A.; and La Tegola, A., "A Modified Pull-Out Test for Bond of Near-Surface Mounted FRP Rods in Concrete," *Composites. Part B, Engineering*, V. 33, No. 8, 2002, pp. 589-603.

16. Nilson, A. H., "Internal Measurement of Bond Slip," ACI JOURNAL, *Proceedings* V. 69, No. 7, July 1972, pp. 439-441.

17. Taher Khorramabadi, M., "FRP Bond Behaviour during Intermediate Concrete Cover Separation in Flexurally Strengthened RC Beams," PhD thesis, University of Cambridge, Cambridge, UK, 2010.